



Flavocytochrome P450 BM3 mutant W1046A is a NADH-dependent fatty acid hydroxylase: Implications for the mechanism of electron transfer in the P450 BM3 dimer

Hazel M. Girvan^a, Adrian J. Dunford^a, Rajasekhar Neeli^a, Idorenyin S. Ekanem^b, Timothy N. Waltham^a, M. Gordon Joyce^c, David Leys^a, Robin A. Curtis^b, Paul Williams^a, Karl Fisher^a, Michael W. Voice^d, Andrew W. Munro^{a,*}

^a Manchester Interdisciplinary Biocentre, Faculty of Life Sciences, University of Manchester, 131 Princess Street, Manchester M1 7DN, UK

^b School of Chemical Engineering and Analytical Science, University of Manchester, 131 Princess Street, Manchester M1 7DN, UK

^c Department of Biochemistry, University of Leicester, Henry Wellcome Building, Lancaster Road, Leicester LE1 9HN, UK

^d Cypex Ltd., 6 Tom McDonald Avenue, Dundee DD2 1NH, UK

ARTICLE INFO

Article history:

Available online 22 September 2010

Keywords:

Cytochrome P450
Flavocytochrome P450 BM3
Electron transfer
FMN dissociation
Fatty acid hydroxylation
Coenzyme selectivity

ABSTRACT

Bacillus megaterium P450 BM3 (BM3) is a P450/P450 reductase fusion enzyme, where the dimer is considered the active form in NADPH-dependent fatty acid hydroxylation. The BM3 W1046A mutant was generated, removing an aromatic “shield” from its FAD isoalloxazine ring. W1046A BM3 is a catalytically active NADH-dependent lauric acid hydroxylase, with product formation slightly superior to the NADPH-driven enzyme. The W1046A BM3 K_m for NADH is 20-fold lower than wild-type BM3, and catalytic efficiency of W1046A BM3 with NADH and NADPH are similar in lauric acid oxidation. Wild-type BM3 also catalyzes NADH-dependent lauric acid hydroxylation, but less efficiently than W1046A BM3. A hypothesis that W1046A BM3 is inactive [15] helped underpin a model of electron transfer from FAD in one BM3 monomer to FMN in the other in order to drive fatty acid hydroxylation in native BM3. Our data showing W1046A BM3 is a functional fatty acid hydroxylase are consistent instead with a BM3 catalytic model involving electron transfer within a reductase monomer, and from FMN of one monomer to heme of the other [12]. W1046A BM3 is an efficient NADH-utilizing fatty acid hydroxylase with potential biotechnological applications.

© 2010 Elsevier Inc. All rights reserved.

Introduction

The cytochromes P450 (P450s) are heme *b*-containing enzymes, the vast majority of which catalyze the reductive activation of dioxygen bound to the heme iron, and the insertion of a single atom of oxygen into a substrate molecule bound close to the heme in the P450 active site. A cysteine thiolate proximal ligand is found in all P450s, with a water (or hydroxide ion) usually located as the distal ligand in the resting ferric form, and with this being replaced by dioxygen on heme reduction and catalytic cycle initiation [1,2]. The P450s were the original enzyme “superfamily” and their numbers continue to expand with ongoing genome sequencing efforts (e.g. 20 P450s in *Mycobacterium tuberculosis* and >250 P450s in *Arabidopsis thaliana*) [3,4].

A schism in the P450 superfamily occurs between eukaryotic and prokaryotic P450s, with the former being soluble enzymes and the latter being membrane associated via a N-terminal trans-

membrane anchor region [5]. This has meant that the prokaryotic P450s have historically proven more amenable to high level expression and purification, leading to structural characterization by X-ray crystallography. As a consequence, selected bacterial P450s are among the most intensively analyzed P450 isoforms, with the camphor hydroxylase P450cam (CYP101A1) from *Pseudomonas putida* and the fatty acid hydroxylase P450 BM3¹ (CYP102A1) from *Bacillus megaterium* being arguably the best studied of all the P450s [6,7]. P450 BM3 (BM3) has a particularly important position in the P450 superfamily as the first example of a bacterial P450 that uses a eukaryotic-like redox partner (the FAD- and FMN-binding enzyme NADPH-cytochrome P450 reductase, CPR) and the first P450 enzyme found fused to its redox partner [7,8]. BM3 is a 119 kDa P450-CPR fusion that has the highest

¹ Abbreviations used: BM3 or P450 BM3, flavocytochrome P450 BM3 from *Bacillus megaterium*; BSTFA, *N,O*-bis(trimethylsilyl)trifluoroacetamide; CO, carbon monoxide; CPR, NADPH-cytochrome P450 reductase; KPi, potassium phosphate; NAD(P)H, either NADH or NADPH; NO, nitric oxide; NOS, nitric oxide synthase; P450, cytochrome P450; TMCS, trimethylchlorosilane; WT, wild-type.

* Corresponding author. Fax: +44 161 306 4192.

E-mail address: Andrew.Munro@Manchester.ac.uk (A.W. Munro).

turnover number reported for a P450 oxygenase enzyme (*ca* 280 s⁻¹ with arachidonic acid), and the wild-type (WT) BM3 catalyzes hydroxylation of long chain fatty acids, predominantly at the ω -1 to ω -3 positions [9,10].

Studies by Black and co-workers highlighted that BM3 had a quaternary structure, unlike any previously characterized bacterial P450 enzyme [11]. In their study, gel filtration analysis indicated that dimer as well as a number of higher oligomeric species could be observed. Neeli et al. provided initial evidence that the dimeric form of BM3 was the catalytically relevant fatty acid hydroxylase species, with studies that included the demonstration that catalytically inactive point mutant enzymes A264H (in which the His264 coordinates the heme iron to occlude the oxygen binding site) and G570D (in which FMN binding is abolished) could be reconstituted to regenerate fatty acid hydroxylase activity [12]. The conclusion from the mutant studies was that electron transfer should occur from NADPH to FAD and then FMN within one monomer (A264H), and then from this FMN across to the heme in the second monomer (G570D) within the dimer (Fig. 1). This model of electron transfer within a flavocytochrome dimer is the same as that proposed to occur in nitric oxide synthase (NOS), which is also formed from the fusion of a CPR-like module to a heme thiolate protein that catalyzes successive oxidations of L-arginine to generate L-citrulline and nitric oxide (NO) as a signaling molecule [13,14]. Subsequently, Kitazume et al. also concluded that the BM3 dimer was the functionally relevant species, but suggested that electron transfer could occur from the FAD of monomer 1 to the FMN of monomer 2, and then either back to the heme of monomer 1 or on to the heme of monomer 2 within the dimer [15]. This conclusion was also based on studies of mutant complementation to restore activity in heterodimeric enzymes, with the F87Y mutant in the heme domain considered as inactive in fatty acid oxidation (through disruption of P450 active site structure) and the W1046A mutant considered “inactive” due to alterations in the vicinity of the FAD cofactor. However, in

the presence of NPG substrate and NADPH (but not NADH), the oxygen consumption rates in the F87Y and W1046A mutants were substantially greater than for their respective double mutants in combination with G570D [15]. The G570D point mutant of P450 BM3 was shown to have no measurable FMN content or myristic acid hydroxylase activity in studies of Klein and Fulco [16], and thus there appeared a likelihood that fatty acid oxidase activity might be retained in one or both of the W1046A and F87Y BM3 mutants.

WT P450 BM3, like CPR and other members of the diflavin reductase enzyme family, shows a strong selectivity for NADPH over NADH as its reducing coenzyme. The specificity constant (k_{cat}/K_m) in cytochrome *c* reduction assays is $\sim 262 \mu\text{M}^{-1} \text{min}^{-1}$ with NADPH as the reducing coenzyme and $\sim 0.06 \mu\text{M}^{-1} \text{min}^{-1}$ with NADH in WT human CPR (i.e. an approximately 4370-fold difference in favor of NADPH) [17]. In previous studies, Döhr and co-workers generated the W676H and W676A mutants of human CPR, where this tryptophan occupies the same position as W1046 in P450 BM3 reductase with its aromatic side chain covering the *re*-face of the FAD isoalloxazine ring. Importantly, Döhr et al. showed that the W676A mutation effected a considerable (~ 1090 -fold) switch in coenzyme specificity from NADPH towards NADH, and enabled the W676A CPR enzyme not only to function efficiently as a reductase of ferricyanide and cytochrome *c*, but also to support catalytic function of the human CYP1A2 enzyme [17]. While Kitazume et al. considered that the P450 BM3 W1046A mutant “should lack NADPH-dependent activity”, evidence for absence of fatty acid hydroxylation was not presented. Our own previous studies on the W1046A mutant in the CPR domain of BM3 (residues 473–1048 of the 1048 amino acid protein) and in the smaller FAD/NADPH-binding (ferredoxin reductase-like) domain of BM3 (residues 664–1048) showed that the W1046A mutation (as did the W676A mutant of human CPR) induced a substantial switch in coenzyme selectivity towards NADH in both the BM3 W1046A CPR and FAD/NADPH domain enzymes [18]. The shifts in catalytic efficiency towards NADH (measured as the ratio of specificity constants, k_{cat}/K_m values, for NADH-dependent versus NADPH-dependent activities) were ~ 1710 -fold relative to WT for the W1046A reductase in cytochrome *c* reduction and >5700 -fold in ferricyanide reduction, even greater coenzyme specificity switches than were reported for the comparable W676A mutant of human CPR [17,18].

In view of our preceding data and the absence of specific evidence for the inactivity (or otherwise) of the W1046A flavocytochrome P450 BM3 in fatty acid hydroxylation, we decided to characterize this mutant of the full length P450 BM3 in order to establish its spectroscopic and kinetic properties, and its competence as a NADPH- and NADH-dependent fatty acid hydroxylase. The data presented in this paper demonstrate that W1046A P450 BM3 is a functional fatty acid oxidase with either NADH or NADPH (NAD(P)H) as reductant, providing further support to our previous model of NOS-like FMN (monomer 1)-to-heme (monomer 2) electron transfer to support catalytic function in the catalytically relevant P450 BM3 dimer. We also present data demonstrating that FMN dissociation occurs in P450 BM3 and its reductase domain as a consequence of its extended incubation at low concentrations, and that this flavin dissociation results in loss of cytochrome *c* reductase activity. These data also have important ramifications for the development of a model of electron transfer in the flavocytochrome P450 BM3 dimer, since previous studies by Kitazume et al. resulted in the hypothesis that loss of cytochrome *c* reductase activity during such incubations may instead be purely a consequence of BM3 dimer dissociation [15]. Collectively, the data presented are consistent with our earlier studies on the BM3 dimer and inter-monomer electron transfer, and simultaneously highlight the production of an efficient, NADH-specific variant of the P450 BM3 fatty acid hydroxylase enzyme.

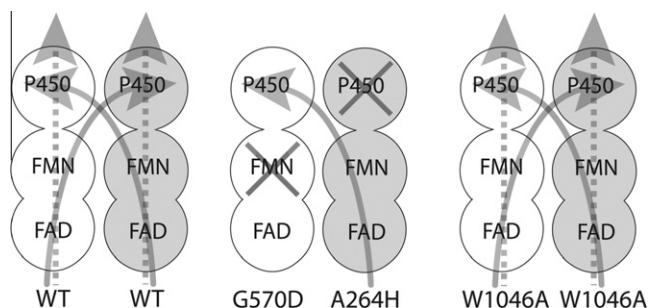


Fig. 1. Schematic of putative electron transfer pathways in flavocytochrome P450 BM3. The dimeric form of P450 BM3 is required for efficient fatty acid hydroxylase activity. The left side panel illustrates the organization of FAD and FMN cofactors (in the CPR domain) and arrows indicate possible directions of NAD(P)H-derived electron transfer through FAD and FMN to the heme iron in the P450 domain. The most plausible electron transfer routes are either directly through cofactors within each monomer (dotted arrows) or from the FMN cofactor in one monomer (FMN₁) to the heme iron in the other (heme₂) (solid arrows), as appears to be the case in the eukaryotic nitric oxide synthase (NOS) flavocytochromes [13]. The central panel shows the NOS-like electron transfer pathway predicted in the heterodimer of G570D and A264H mutants of P450 BM3. The former mutation prevents FMN binding while the latter has His264 as a 6th ligand to the P450 heme iron. Both mutants are inactive as fatty acid hydroxylases, but activity is recovered in the heterodimer, consistent with FMN₁-to-heme₂ electron transfer [12,38]. The right side panel shows WT-like potential electron transfer pathways in the W1046A BM3 mutant. Data presented in this study demonstrate that this mutant enzyme is active in fatty acid hydroxylation, contrary to conclusions made in a previous study [15]. In light of previous studies of the G570D/A264H mutants, the FMN₁-to-heme₂ electron transfer model is also favoured for the W1046A BM3 mutant.

Materials and methods

Generation of the W1046A mutant in flavocytochrome P450 BM3

The production of the W1046A variant of the P450 BM3 reductase domain was described in our previous publication [18]. Site-directed mutagenesis to create the W1046A mutant of intact flavocytochrome P450 BM3 was carried out as described previously, using the QuikChange method (Stratagene) and the aforementioned primers [18]. The WT flavocytochrome P450 BM3 (*CYP102A1*) gene was used as the template in the expression plasmid pBM25 [19]. Introduction of the required mutation and the absence of undesired secondary mutations were verified by DNA sequencing of the full gene (GeneService, London, UK).

Expression and purification of W1046A and WT flavocytochromes P450 BM3, and the WT BM3 reductase domain

The WT and W1046A flavocytochromes P450 BM3 were expressed in *Escherichia coli* strain TG1. Cells were grown in Terrific Broth at 37 °C, harvested and lysed as described previously [9,20]. Enzymes were purified by successive chromatographic steps using DEAE- and Q-Sepharose, followed by hydroxyapatite chromatography and a final gel filtration step on Sephacryl S-200, as previously [20,21]. The WT BM3 reductase domain was expressed and purified as before [18]. EDTA (1 mM) and the protease inhibitors phenylmethanesulfonyl fluoride (PMSF, 1 mM) and benzamide hydrochloride (1 mM) were kept in all buffers during purification steps for the proteins. Concentrations for the oxidized forms of purified WT and W1046A flavocytochromes P450 BM3 were determined using the coefficient $\epsilon_{418} = 105 \text{ mM}^{-1} \text{ cm}^{-1}$, and for the oxidized form of the WT reductase domain using $\epsilon_{456} = 21.2 \text{ mM}^{-1} \text{ cm}^{-1}$, as described previously [9,19,22,23].

UV-visible absorbance and substrate binding analysis of P450 enzymes

All UV-visible absorbance measurements to analyze spectral properties of the WT and W1046A variant of flavocytochrome P450 BM3, and the WT BM3 CPR domain were done using a Cary 50 UV-visible scanning spectrophotometer (Varian) and 1 cm pathlength quartz cuvettes. Analysis of the binding of arachidonic acid, lauric acid, and *N*-palmitoylglycine (NPG) to the W1046A BM3 enzyme as well as NAD(P)H-dependent reduction and sodium dithionite reduction/CO (carbon monoxide)-binding assays were done as previously [9,18]. Unless otherwise stated, assays were done in standard assay buffer (50 mM potassium phosphate [KPi], pH 7.0) at 25 °C. Spectral data fitting was done as previously described, and using Origin software (OriginLab, Northampton, MA).

Steady-state fatty acid turnover assays with WT and W1046A flavocytochromes P450 BM3

The steady-state turnover of selected fatty acids (lauric acid and *N*-palmitoylglycine [NPG]) was monitored indirectly by oxidation of NADPH and NADH coenzymes on a Cary 50 spectrophotometer, and using $\Delta\epsilon_{340} = 6.21 \text{ mM}^{-1} \text{ cm}^{-1}$. The k_{cat} and K_{m} values were determined with flavocytochrome enzymes (WT and W1046A) typically at 450 nM, fatty acids (NPG at 50 μM , lauric acid at 500 μM) and NAD(P)H varied across a range up to $\sim 1.5 \text{ mM}$. Plots of specific rates at different NAD(P)H concentrations were fitted to the Michaelis–Menten equation to define apparent k_{cat} and K_{m} parameters in each case, using Origin software. Assays were done in assay buffer at 25 °C.

Stopped-flow analysis of heme iron reduction in WT and W1046A flavocytochromes P450 BM3

Apparent flavin-to-heme electron transfer rates were measured by stopped-flow absorbance spectroscopy using an Applied Photophysics SX18 MVR stopped-flow spectrophotometer contained within an anaerobic glove box (Belle technology) to maintain an oxygen free environment. To measure the rate of flavin (FMN)-to-heme electron transfer, the accumulation of the Fe^{2+} -CO complex of the BM3 heme iron was monitored at 450 nm. All buffers used were degassed and saturated with CO. Enzyme (WT or W1046A BM3, 3 μM) and lauric acid (100 μM) pre-mixed in the first syringe were then mixed against NAD(P)H (200 μM) in the stopped-flow, and the ΔA_{450} absorption transients collected were fitted using either a monophasic or a biphasic exponential process using the Applied Photophysics software. To examine the effect of pre-incubation of WT and W1046A enzymes with NAD(P)H, sequential mixing experiments were done. Pre-mixed lauric acid (100 μM) and enzyme (3 μM) were first mixed with NAD(P)H (200 μM) and incubated for either 100 ms or 60 s, prior to a second mix with an equal volume of CO-saturated anaerobic buffer. The ΔA_{450} transient data were then fitted using a biphasic exponential function to determine the apparent rate constants for FMN-to-heme electron transfer (k_{red}).

Analysis of flavin fluorescence and cytochrome *c* reductase activity in diluted samples of WT flavocytochrome P450 BM3 and its CPR domain

WT P450 BM3 and its CPR domain were incubated in either 5 mM KPi (pH 7.4) or 50 mM KPi (pH 7.4) in stock solutions at various concentrations in the range between 25 nM and 3 μM at 25 °C for a period of 1 h, and as described by Kitazume et al. [15]. Thereafter, samples were taken from the incubations and assayed directly (in the case of the 25 nM sample) or diluted to a final concentration of 25 nM from the other samples into the same buffer. They were then assayed for cytochrome *c* reductase activity at 25 °C by addition of cytochrome *c* (35 μM) and NADPH (200 μM), and by following A_{550} change ($\Delta\epsilon_{550} = 22.64 \text{ mM}^{-1} \text{ cm}^{-1}$) on reduction of the cytochrome *c* heme iron from ferric to ferrous [9]. In parallel, the flavin fluorescence was measured in the final 25 nM samples (with no further additions) with excitation at 450 nm and emission spectra collected between 490 and 650 nm. Fluorescence spectra were all corrected for Raman scattering by subtraction of a buffer-only spectrum in each case. Samples were then boiled for 5 min, centrifuged in a microfuge at full speed for 1 min, and fluorescence spectra again recorded for the supernatants. Fluorescence spectra were all recorded for samples at 25 °C. UV-visible spectroscopic assays were done on a Cary 50 spectrophotometer (as described above). Fluorescence spectra were recorded on a Cary Eclipse fluorimeter (Varian) using a 1 cm pathlength quartz fluorescence cuvette and with excitation and emission slits both set to 20 nm.

Fatty acid product characterization from lauric acid oxidation by WT and W1046A P450 BM3 enzymes

Analysis of oxygenated products from NAD(P)H-dependent turnover of lauric acid by both WT and W1046A flavocytochromes P450 BM3 was done both using LC with radiometric detection of ^{14}C labeled lauric acid and by GC-MS on unlabeled lauric acid following derivatization of reaction products using BSTFA [*N*,*O*-bis(trimethylsilyl)trifluoroacetamide] and TMCS (trimethylchlorosilane). For the radiolabelled lauric acid assays, 1 μM WT or W1046A P450 BM3 (2 μl volumes) was added to 158 μl of pre-mixed (873 μM lauric acid, 12.7 μM ^{14}C lauric acid) in 100 mM potassium phosphate, pH 7.4. This was incubated at 37 °C for

1 min prior to addition of coenzyme (40 μ l of 5 mM NAD(P)H or NADP⁺ as control). A control reaction was also done using the FMN-free G570D mutant. Incubations were continued for various points up to 2 min, and then stopped by addition of 25 μ l of 1 M HCl. The samples were centrifuged in a microfuge at 13,000 rpm for 10 min, and supernatants analyzed by HPLC. Samples were resolved using an Agilent 1100 system on a Phenomenex hyperclone 3 μ m C18 ODS column (150 \times 3.2 mm) with radiometric detection using solid scintillant. Reactions for GC-MS analysis were done using 1 μ M enzyme and 700 μ M sodium dodecanoate (lauric acid). Reactions were also done with 300 μ M *n*-palmitoylglycine (NPG), along with negative controls run in absence of added lipid substrate or coenzyme. Reactions were in assay buffer and started by addition of NAD(P)H (1 mM) with stirring at 25 $^{\circ}$ C. Reactions were terminated at 10 s, 30 s, or 2 min by acidification with HCl, as above. Thereafter, oxidized samples were isolated, derivatized, and resolved as described in our previous work [24]. Total abundance of different products (ω -1, ω -2, and ω -3 hydroxy fatty acids) was determined by integration of product peaks using system software.

Materials

¹⁴C-labeled lauric acid was from Cypex (Dundee, UK). Bacterial growth medium (Tryptone, yeast extract) was from Melford Laboratories (Ipswich, Suffolk, UK). Unless otherwise state, all other reagents were from Sigma-Aldrich and were of the highest grade available.

Results

Expression, purification, and optical properties of the P450 BM3 W1046A mutant

The W1046A mutation was successfully introduced into the intact flavocytochrome P450 BM3 enzyme, and the mutant enzyme isolated according to previously described methods [17,19,20]. The purified enzyme exhibited optical properties near-identical to those for the WT BM3. The P450 is extensively low-spin (LS) with its Soret band at 418.5 nm, and the absence of any significant high-spin (HS) feature at \sim 390 nm. The alpha and beta bands of the W1046A BM3 heme are located at 569 and 535 nm, respectively. The presence of flavin cofactors (FAD and FMN) is evident from the substantial spectral contribution in the region between 450 and 540 nm, consistent with the spectral properties of the oxidized WT P450 BM3 [19] (Fig. 2A). Previous studies of the W1046A CPR and FAD/NADPH binding domain indicated that the FAD and FMN cofactors were incorporated to the same levels as the WT proteins, and also that these mutant enzymes had high activity in both cytochrome *c* reductase and potassium ferricyanide reductase assays [12]. Thus, preceding data were consistent with efficient NAD(P)H-dependent electron transfer to substrates that receive electrons mainly from either the FAD (ferricyanide) and the FMN (cytochrome *c*) cofactors. Addition of either NADPH or NADH to the W1046A flavocytochrome resulted in the same extent of spectral bleaching in the 450–540 nm region, consistent with substantial reduction of the flavin cofactors (Fig. 2A). The absence of any significant change in absorbance in the 600 nm region on P450 BM3 W1046A reduction by NAD(P)H is indicative of a lack of accumulation of the neutral (blue) semiquinone form of the FAD. Previous studies of the W1046A CPR and FAD/NADPH binding domains showed that this mutation destabilized the FAD blue semiquinone (formed in the WT enzymes) in favor of the 2-electron reduced hydroquinone FAD form [18]. Spectral data for the W1046A P450 BM3 enzyme indicate that this property is retained in the intact

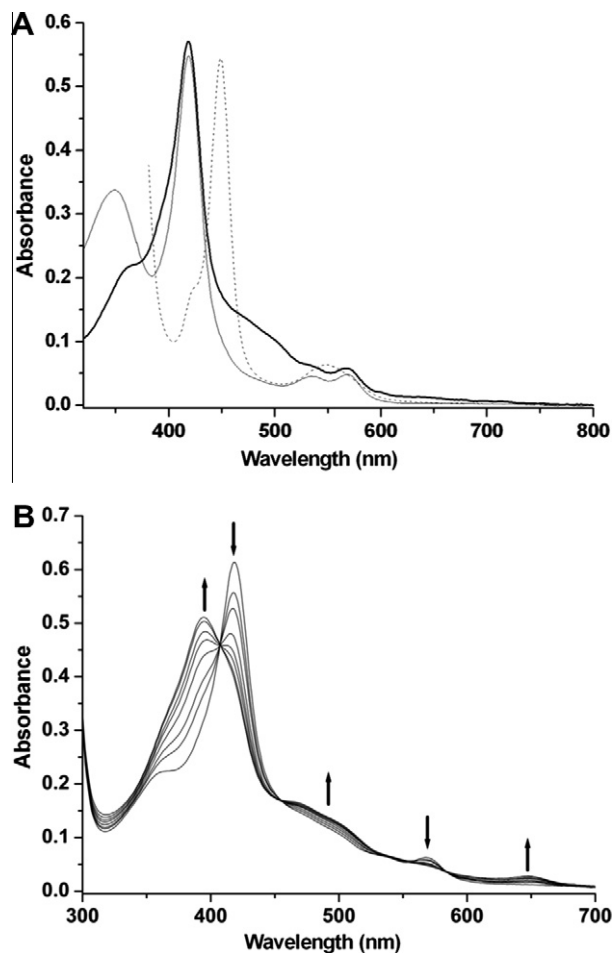


Fig. 2. UV-visible spectroscopic properties of the P450 BM3 W1046A mutant. (A) Absorbance spectra for oxidized (thick solid line), NADH-reduced (75 μ M, thin solid line), and sodium dithionite-reduced and CO-bound (dashed line) forms of the BM3 W1046A enzyme (5.5 μ M). There is no significant NAD(P)H-dependent formation of the Fe²⁺-CO complex of the BM3 W1046A enzyme in the absence of fatty acid substrate. (B) Absorbance spectrum for oxidized, substrate-free W1046A P450 BM3 (5.9 μ M, spectrum with greatest intensity at 418.5 nm), accompanied by selected spectra from the titration of the enzyme with arachidonic acid. The final spectrum shown (8.25 μ M arachidonic acid) has absorbance maximum at 394 nm. Arrows indicate directions of absorbance change on arachidonic acid addition at selected points in the W1046A BM3 UV-visible spectrum.

flavocytochrome (Fig. 2A). In common with the WT P450 BM3 enzyme, there is no significant formation of the Fe²⁺-CO complex on addition of carbon monoxide to the NAD(P)H-reduced W1046A P450 BM3 enzyme, demonstrating that these coenzymes reduce the flavin cofactors, but not the heme iron. Conversion to a Fe²⁺-CO species with spectral maximum at 448 nm is achieved using sodium dithionite as a reductant. The spectrum of the W1046A CO complex demonstrates retention of cysteine thiolate as the proximal ligand to the heme iron in this variant BM3 enzyme, as might be expected for a mutation distant from the heme binding site (Fig. 2A).

To demonstrate typical substrate-induced optical changes in the W1046A BM3 heme, binding of various BM3 fatty acid substrates (e.g. lauric acid, NPG, arachidonic acid) was done, and in each case W1046A heme spectral changes occurred that were consistent with a shift in ferric heme iron spin-state equilibrium from low-spin to high-spin. Fig. 2B shows results from a spectral titration of the BM3 W1046A enzyme with arachidonic acid. There is a progressive shift in the Soret maximum from 418.5 to 394 nm as arachidonic acid binds, along with the development of a charge

transfer band at 648 nm that is typical for substrate-bound P450s. A data fit for the arachidonic acid-induced change in the heme spectrum produces a K_d value of $0.24 \pm 0.07 \mu\text{M}$, consistent with previously reported values for the WT P450 BM3 enzyme (e.g. $0.55 \mu\text{M}$) [9,24]. The W1046A BM3 K_d values for lauric acid and NPG were $216 \pm 14 \mu\text{M}$ and $0.13 \pm 0.01 \mu\text{M}$, respectively. These are similar to values reported previously for the binding of these lipids to WT P450 BM3, suggesting that active structure in the BM3 heme domain is not influenced substantially by the W1046A mutation in the FAD/NADPH binding domain [25,26]. Overall, W1046A BM3 spectral data indicate the enzyme has full heme and flavin cofactor content, and that it undergoes coenzyme reduction, substrate binding, and CO complexation reactions typical of the WT enzyme.

Steady-state kinetic analysis of the W1046A flavocytochrome P450 BM3 enzyme

To determine the apparent kinetic parameters for substrate turnover by the W1046A flavocytochrome P450 BM3, the substrates lauric acid and NPG were analyzed. Substrates were kept at near-saturating concentrations, and substrate-dependent oxidation of NADPH and NADH coenzymes was measured at 340 nm. Table 1 presents the apparent k_{cat} and K_m parameters from these studies. For the WT P450 BM3 enzyme, the k_{cat} values are an order of magnitude greater with NADPH than with NADH, and the K_m values for the coenzymes are substantially in favor of NADPH. For instance, with NPG as substrate the K_m is >180-fold lower for WT BM3 with NADPH ($3.4 \mu\text{M}$) than with NADH ($625 \mu\text{M}$). However, there are striking differences in the catalytic parameters with the W1046A BM3 mutant. While the W1046A k_{cat} values with NADPH as reducing coenzyme are lower than those for WT P450 BM3 (~12.5-fold and 8-fold with lauric acid and NPG, respectively), the k_{cat} value with NADH is comparable to that for WT with lauric acid as substrate, and ~9-fold higher with NPG. Moreover, the W1046A K_m values for NADH ($11.5 \mu\text{M}$ with lauric acid, $62 \mu\text{M}$ with NPG) are substantially lower than those for the WT BM3 with the same substrates (20-fold and 10-fold, respectively) (Table 1). Using the specificity constant (k_{cat}/K_m) as a measure of relative efficiency of the WT and W1046A BM3 enzymes with NADPH, there are apparent ~16.7-fold and 11.3-fold decreases in efficiency of the W1046A mutant (cf. WT) with lauric acid and NPG, respectively. However, with NADH as the reducing coenzyme there are ~13.0-fold and 91.4-fold increases in efficiency (cf. WT) with lauric acid and NPG, respectively.

Stopped-flow absorbance analysis of heme iron reduction in WT and W1046A flavocytochromes P450 BM3

Early studies on the P450 BM3 system from Fulco's group demonstrated that NADPH was the preferred coenzyme to support BM3's fatty acid hydroxylase activity [27]. However, both NADPH and NADH are able to transfer electrons to P450 BM3, as shown by the ability of these coenzymes to effect a similar level of reduction of the WT and W1046A BM3 flavin cofactors at equilibrium

(Fig. 2A), in addition to evidence provided from our previous studies on the WT and W1046A CPR and FAD/NADPH binding domains [18]. There are alterations in the relative potentials of the oxidized/semiquinone (ox/sq, 0- to 1-electron reduced) and semiquinone/hydroquinone (sq/hq, 1- to 2-electron reduced) couples of the FAD cofactor in the W1046A mutant as a consequence of the removal of the "shielding" tryptophan 1046 side chain over the FAD isoalloxazine ring. As a result, the equilibrium level of NAD(P)H-dependent FAD reduction is predominantly to the semiquinone (1-electron reduced) in the WT, and to the hydroquinone in the W1046A mutant [18]. To examine the influence of the W1046A mutation on the apparent rate of NAD(P)H-dependent electron transfer to the BM3 heme iron, we measured the rate of formation of the heme Fe^{2+} -CO complex following reduction of lauric acid-bound WT and W1046A BM3 enzymes with NAD(P)H in CO-saturated, anaerobic buffer, and as described in Materials and methods. Studies of the influence of brief (100 ms) and extended (60 s) pre-incubation of enzymes with NAD(P)H were also done, in light of the kinetic preference for BM3 heme iron reduction by the short-lived FMN anionic radical species, and the known accumulation of the FMN hydroquinone (a much poorer reductant of the heme) on incubation of WT BM3 (or its CPR domain) with NADPH in the absence of fatty acid substrate or other electron acceptor, such as cytochrome c [28,29]. Data from these experiments are shown in Table 2.

The results show that electron transfer occurs from both NADH and NADPH coenzymes through the FAD and FMN cofactors, and to the heme iron in both the WT and W1046A flavocytochromes, leading to CO binding to the ferrous heme iron and accumulation of absorbance at 450 nm associated with the characteristic P450 form of this cysteine thiolate coordinated enzyme [30]. In all cases, near-complete accumulation of the P450 Fe^{2+} -CO complex occurred, albeit with widely varying rate constants according to enzyme, reductant and pre-incubation with coenzyme (Table 2). In all but one case, reaction transients fitted best to biphasic exponential processes, with amplitudes of absorbance similar in both the fast and slow phases of the reactions. In all cases, observed rate constants (k_{red}) reported are the averages of at least three individual transients that varied by <5% from the averages reported in Table 2. In recent fast reaction studies using laser excitation methods, we demonstrated that CO binding to ferrous P450 BM3 heme iron occurs with a rate constant in excess of 1000 s^{-1} at saturating CO conditions in solution. This is much faster than BM3 heme iron reduction by electron transfer from the FMN cofactor and thus unlikely to be a rate-limiting factor in the CO complex formation [31]. In previous stopped-flow studies of WT P450 BM3, we reported that the observed rate constant for CO complex formation is $\sim 224 \text{ s}^{-1}$ for myristic acid-bound P450 BM3 reduced by near-saturating NADPH ($500 \mu\text{M}$). We concluded that the first FMN-to-heme electron transfer was a major rate-limiting step in the P450 BM3 catalytic cycle, since 224 s^{-1} is close to the apparent k_{cat} for arachidonic acid oxidation (285 s^{-1}) under similar conditions [9,23]. In the current study (Table 2), data are again consistent with this conclusion, with the fast phase of NADPH-dependent heme reduction ($k_{\text{red}} 1$) for WT BM3 (without coenzyme pre-incubation) being

Table 1

Steady-state kinetic parameters for substrate-dependent NAD(P)H oxidation in WT and W1046A flavocytochrome P450 BM3 enzymes. Experiments were done as detailed in Materials and methods.

Substrate	P450 BM3 WT				P450 BM3 W1046A			
	NADPH		NADH		NADPH		NADH	
	k_{cat} (min^{-1})	K_m (μM)	k_{cat} (min^{-1})	K_m (μM)	k_{cat} (min^{-1})	K_m (μM)	k_{cat} (min^{-1})	K_m (μM)
Lauric acid	1040 ± 96	6.5 ± 2.5	106 ± 24	228 ± 107	83.5 ± 18	8.7 ± 0.6	69.5 ± 4	11.5 ± 2.5
NPG	1343 ± 97	3.4 ± 1.1	80 ± 15	625 ± 170	172 ± 7	4.9 ± 1.0	726 ± 59	62 ± 13

Table 2
Stopped-flow kinetic data for NADPH- and NADH-dependent heme iron reduction in WT and W1046A flavocytochrome P450 BM3 enzymes. The parameters $k_{\text{red 1}}$ and $k_{\text{red 2}}$ relate to rate constants for the fast and slow phases from fits of ΔA_{450} reaction progress curves with a double exponential function. In the case of the W1046A BM3 mutant with NADPH (and in absence of pre-incubation with coenzyme), reaction transients were monophasic. The absorbance increase at 450 nm relates to electron transfer to the heme iron and the rapid binding of CO to the ferrous heme to form the archetypal cysteine thiolate-coordinated Fe^{2+} -CO P450 complex. Reactions were initiated either by (i) direct mixing of lauric acid-bound BM3 enzymes with NAD(P)H in CO-saturated buffer, or by (ii) pre-mixing lauric acid-bound BM3 enzymes with NAD(P)H in degassed buffer for 100 ms or 60 s prior to a second stopped-flow mix with CO-saturated buffer, as described in Materials and methods.

Coenzyme pre-incubation time	Coenzyme	P450 BM3 WT		P450 BM3 W1046A	
		$k_{\text{red 1}}$ (s^{-1})	$k_{\text{red 2}}$ (s^{-1})	$k_{\text{red 1}}$ (s^{-1})	$k_{\text{red 2}}$ (s^{-1})
0	NADH	52.3	12.8	18.1	3.8
	NADPH	291	33.0	4.5	–
100 ms	NADH	35.9	4.0	14.7	1.8
	NADPH	61.4	6.1	16.0	3.9
60 s	NADH	0.012	0.003	0.0075	0.001
	NADPH	0.013	0.003	0.0105	0.0015

291 s^{-1} . The comparable WT rate with NADH reductant is lower at 52.3 s^{-1} , but clearly demonstrates that reduction of the fatty acid-bound BM3 heme is feasible with NADH (Fig. 3). Rates are slower again in the W1046A mutant, but reduction is apparently faster with NADH (18.1 s^{-1}) than with NADPH (4.5 s^{-1}), and the ΔA_{450} transients are also essentially monophasic in W1046A with NADPH as reductant. Following a short (100 ms) pre-incubation with reducing coenzyme, the WT BM3 heme reduction rates are slowed to 61.4 s^{-1} (NADPH) and 35.9 s^{-1} (NADH), which would be consistent with accumulation of the FMN hydroquinone in this timescale. For W1046A BM3, a 100 ms pre-incubation with NADH decreases the heme reduction rate by $\sim 20\%$ to 14.7 s^{-1} . However, with NADPH the apparent rate is increased (16.0 s^{-1}) and reaction transients become biphasic again. Closer inspection of the data recorded for NADPH-dependent W1046A heme reduction reveals a short lag phase for reaction transients in absence of pre-incubation with coenzyme (20–30 ms) that is much less pronounced in the other comparable transients in absence of coenzyme pre-mixing (Fig. 3) and barely discernible for any of the reaction transients following the 100 ms pre-incubation with NADPH. Possibly, the apparent lag phase and slower electron transfer rate in the non-pre-incubated reaction is due to the formation of a charge transfer (CT) complex between NADP^+ and hydroquinone FAD (FADH_2) in

W1046A BM3 that precedes formal FAD reduction and oxidized coenzyme release. Such phenomena were observed previously in stopped-flow reduction of W1046A FAD/NADPH and CPR domains [18]. The movement of the indole side chain of Trp1046 is required to enable binding of the nicotinamide portion of NAD(P)H close to the FAD isoalloxazine ring and in order for electron (formally hydride ion) transfer, as was shown in studies of the role of Trp676 in human CPR, and further confirmed in studies of the W1046A FAD/NADPH and CPR domain mutants [18,32]. The conclusion that the Trp1046 side chain is also important for displacement of NAD(P)^+ was apparent from the development of CT species in these W1046A domains [18]. The presence of other side chains interacting with the 2'-phosphate group of NAD(P)H (which is absent in NAD(H)) may offer some additional stabilization to the binding of NADP^+ (compared to NAD^+) to explain the brief lag phase in W1046A BM3 heme reduction transients that occur in the absence of pre-incubation with NADPH.

For the WT and W1046A mutants of BM3, extended (60 s) pre-incubation with NAD(P)H leads to a dramatic decrease in heme reduction rate to $\sim 0.01 \text{ s}^{-1}$ ($\sim 6 \text{ min}^{-1}$) in each case. In the anaerobic solutions used for these experiments, there is no possibility of any substantial oxidation of coenzyme in the pre-incubation phase, and this conclusion is also borne out by the fact that the ΔA_{450} transients are of similar final intensity in all of the experimental sets (i.e. near-complete P450 Fe^{2+} -CO complex formation is achieved). The logical conclusion drawn is that the 60 s pre-incubation with NAD(P)H enables the CPR domains of both WT and W1046A flavocytochromes P450 BM3 to become fully loaded with electrons in accordance with the relative reduction potentials of NAD(P)H and the FAD/FMN flavins. Both the FMN ox/sq and sq/hq redox couples and the FAD ox/sq couple are considerably more positive than that for NAD(P)H/NAD(P)^+ (-320 mV versus the normal hydrogen electrode), while the FAD sq/hq couple is slightly more negative in the case of WT BM3, but more positive in the W1046A enzyme [18,28,33]. As a consequence, these equilibrium forms are ones in which the BM3 FAD either populates a mixture of semiquinone and hydroquinone (WT) or is near-fully hydroquinone (W1046A), whereas the FMN is effectively completely in the hydroquinone state in both WT and the W1046A mutant. The FMN hydroquinone is an inferior reductant of the heme (compared to the semiquinone), leading to the much lower rates of Fe^{2+} -CO complex formation observed (Table 2) and converting P450 BM3 to a low activity fatty acid hydroxylase form [8].

Demonstration of NADPH- and NADH-dependent fatty acid hydroxylation in WT and W1046A flavocytochromes P450 BM3

Following the demonstration of NAD(P)H-dependent reduction of the heme iron in both WT and W1046A P450 BM3, we analyzed the capacity of these enzymes to catalyze hydroxylation of lauric

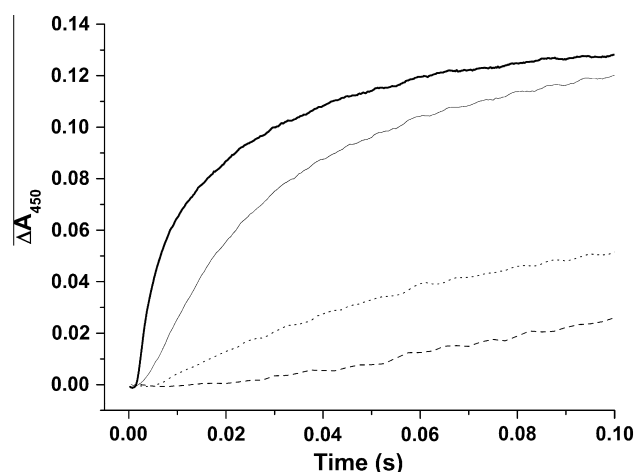


Fig. 3. Stopped-flow absorbance analysis of Fe^{2+} -CO complex formation in WT and W1046A P450 BM3 enzymes. Stopped-flow transients at 450 nm are shown, reporting on heme iron reduction in WT and W1046A P450 BM3, followed by rapid CO binding to form the P450 Fe^{2+} -CO complex. Reactions were done as described in Materials and methods, and without pre-incubation of lauric acid-bound enzymes with NAD(P)H. The thick solid line represents the reduction of WT BM3 with NADPH, and the thin solid line is WT reduced with NADH. The dotted line is W1046A BM3 reduced with NADH and the dashed line is W1046A reduced with NADPH. Rate constants derived from these data are presented in Table 2.

acid using both NADH and NADPH coenzymes as reductants. In preliminary work we examined the enzyme-mediated oxidation of ^{14}C labeled lauric acid by HPLC, as detailed in the Materials and methods section. Using the system described, unconverted lauric acid substrate eluted at ~ 14.6 min, with three products (i.e. the ω -1, ω -2, and ω -3 hydroxylauric acid metabolites) eluting in a closely spaced group at ~ 6.5 – 7.7 min. Products were observed for both WT and W1046A P450 BM3 and with both NADH and NADPH as reductants. While quantification of individual metabolites was difficult due to a lack of resolution in their retention times, what was clear was that the WT BM3 with NADPH reductant was the most efficient hydroxylation system, with $\sim 90\%$ of the substrate converted to hydroxylated products within 30 s. In addition, the W1046A BM3 mutant hydroxylated a greater proportion of lauric acid with NADH coenzyme than did the WT BM3 enzyme over the same time period. In control experiments, it was also established that no oxidized lauric acid products were generated in the absence of enzyme or coenzymes, and that the FMN-free G570D mutant of flavocytochrome P450 BM3 was completely inactive in lauric acid hydroxylation, entirely consistent with our previous studies of BM3 dimer formation [12].

In order to achieve better resolution of the different hydroxylated products and to obtain a more quantitative analysis of their individual abundance, we used GC–MS methods, as described in Materials and methods, and in our previous studies of P450 BM3 [24]. Data from these analyses further confirmed the production of ω -1, ω -2, and ω -3 hydroxylauric acid metabolites from both WT/W1046A BM3 enzymes, and using both NADPH and NADH coenzymes. Fig. 4A shows a typical gas chromatogram of reaction products – in this case from the turnover of lauric acid by the W1046A BM3 enzyme with NADH as the reducing coenzyme. Unconverted lauric acid has a retention time of 11.25 min, and the three expected metabolites of BM3-mediated substrate oxidation are seen at 12.99 min (ω -3 hydroxylauric acid), 13.18 min

(ω -2 hydroxylauric acid), and 13.29 min (ω -1 hydroxylauric acid). Fig. 4B shows the mass spectrum of the product species at 12.99 min, corresponding to the TMS-derivative of ω -3 hydroxylauric acid. Fig. 5 is a scheme showing the proportions of the various ω -1 to ω -3 hydroxylauric acid products generated from the various enzyme/coenzyme combinations in reactions over both 30 s and 2 min. The data here are consistent with those from the HPLC studies reported above, confirming that the WT BM3 with NADPH is the most efficient combination, converting $>90\%$ of lauric acid to hydroxylated products in 30 s. These data thus contradict previous suggestions that the W1046A flavocytochrome BM3 mutant is inactive as a fatty acid hydroxylase [15]. In fact, W1046A BM3 is active with both NADPH and NADH as reductants, and is rather more efficient with NADH as the coenzyme. In the 30 s incubation with NADH, the W1046A BM3 enzyme converts $\sim 69\%$ of lauric acid to the ω -1 to ω -3 hydroxylauric acid products, and this proportion rises to 88% following a 2 min incubation. Also of note is that the WT BM3 enzyme is clearly capable of NADH-dependent lauric acid hydroxylation, albeit less efficiently than the W1046A enzyme driven by NAD(P)H. In turnover driven by NADH, WT BM3 converts $\sim 20\%$ of lauric acid to hydroxylated products in 30 s, increasing to $\sim 52\%$ product formation over 2 min (Fig. 5). In related experiments, we could also demonstrate the NAD(P)H-dependent oxidation of NPG substrate by both WT and W1046A P450 BM3 enzymes. However, in addition to the three products expected (the TMS derivatives of ω -1 to ω -3 NPG), GC–MS revealed a further three products that likely resulted from fragmentation of the former trio of oxidized products at the GC–MS analysis stage, or during derivatization of the products (data not shown). Given that WT BM3 is less efficient in NADH-dependent lauric acid hydroxylation than is W1046A BM3 with NAD(P)H, it appears to be the case that the apparent rates of P450 heme iron reduction (where NADH-dependent heme iron reduction of WT BM3 was faster than NAD(P)H-dependent heme iron reduction in W1046A

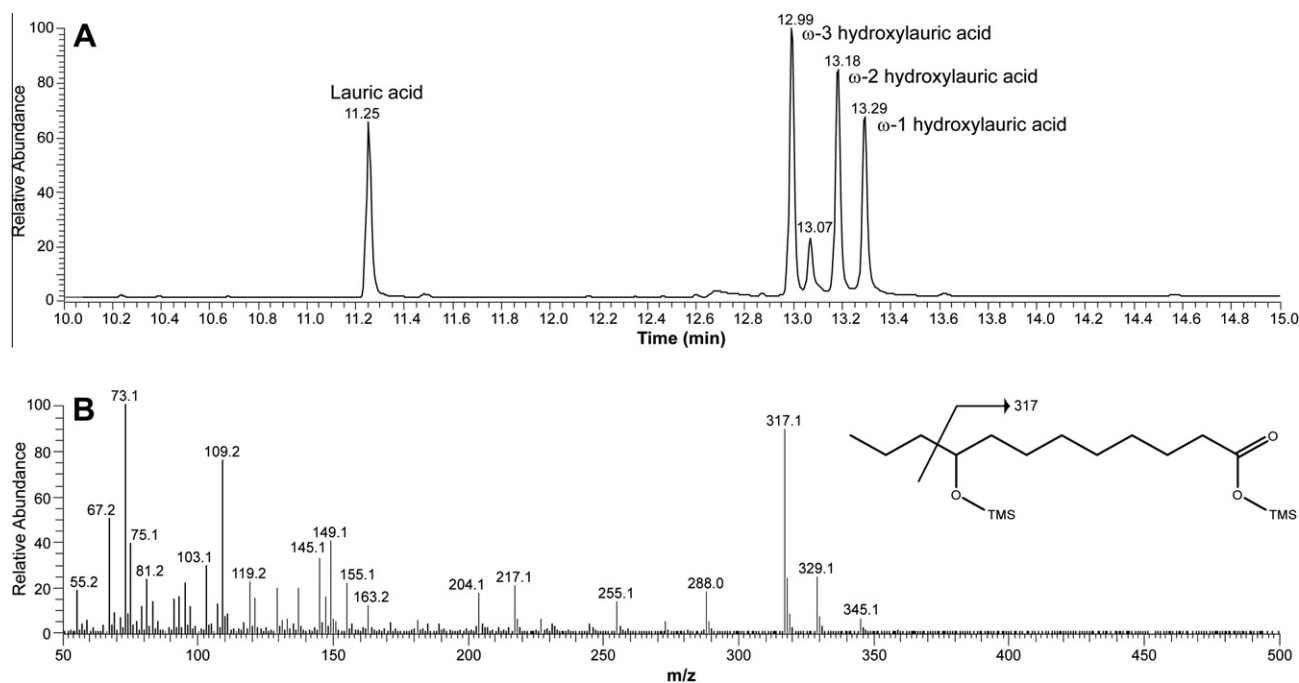


Fig. 4. NADH-dependent hydroxylation of lauric acid catalyzed by the W1046A mutant of flavocytochrome P450 BM3. Panel A shows a gas chromatogram demonstrating formation of ω -1, ω -2, and ω -3 hydroxylauric acid products from lauric acid substrate catalyzed by the W1046A P450 BM3 mutant and with NADH as the reducing coenzyme. Reaction conditions were as described in Materials and methods, and the reaction was stopped after 10 s. Products and unconverted substrate were treated to form TMS derivatives and resolved by gas chromatography, as described previously [24]. The identities of substrate/product peaks and their retention times are indicated. The minor species with retention time of 13.07 min is a contaminant (possibly a plasticizer) that is also observed in negative control reactions where no other products are formed. Panel B shows the mass spectrum of the product species with GC peak retention time of 12.99 min. This product corresponds to TMS derived ω -3 hydroxylauric acid.

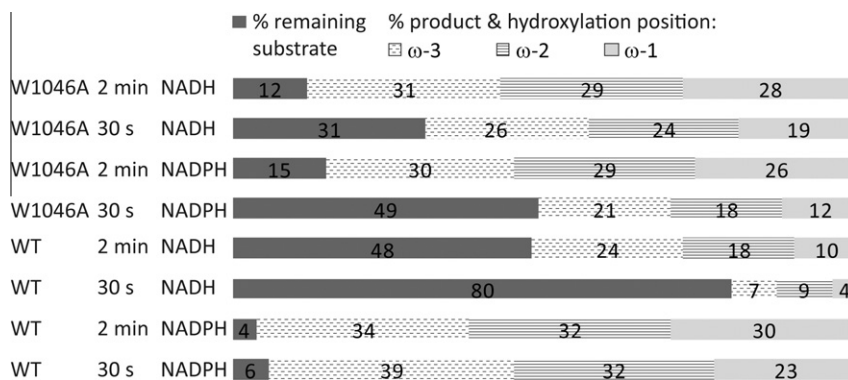


Fig. 5. Proportions of products formed by WT and W1046A BM3-catalyzed lauric acid hydroxylation. The scheme shows the proportions of ω -1, ω -2, and ω -3 hydroxylauric acid products (and unconverted lauric acid substrate) in reactions with WT and W1046A BM3 enzymes using NAD(P)H as reductants. Reactions were done as described in Materials and methods, and stopped after incubation periods of either 30 s or 2 min. The data indicate WT BM3 with NADPH reductant is the most efficient lauric acid hydroxylase, but that the W1046A BM3 mutant with NADH reductant is also an efficient lauric acid hydroxylase, and that WT P450 BM3 also has NADH-dependent fatty acid oxidation activity.

BM3) need not correlate well with fatty acid hydroxylation outcomes (Fig. 3). Thus, WT BM3 is likely to show a greater level of uncoupling of NADH oxidation from hydroxylated product formation than does W1046A BM3 with NAD(P)H coenzymes.

Collectively, this data set demonstrates that (a) WT P450 BM3 is a catalytically functional fatty acid hydroxylase with both NADH and NADPH coenzymes (although NADPH is the preferred reductant); (b) W1046A P450 BM3 is also catalytically active in fatty acid hydroxylation, using both NADPH and NADH, but with a modest preference for NADH; and (c) W1046A P450 BM3 is markedly superior to WT P450 BM3 in NADH-driven fatty acid hydroxylation.

FMN dissociation from P450 BM3 and its CPR domain following extended incubation at low enzyme concentration

The data provided here demonstrating the catalytic competence of the W1046A P450 BM3 enzyme contradict earlier conclusions that this enzyme should be non-functional in fatty acid hydroxylation [15]. In turn, this leads to the requirement for a re-evaluation of the models of electron transport within the P450 BM3 dimer (see Discussion section). In the study of Kitazume et al., it was reported that the specific rate of cytochrome *c* reduction catalyzed by WT P450 BM3 (10–25 nM enzyme in assay) decreased progressively in line with a concentration range (10 nM to 3 μ M) in which the enzyme was pre-incubated in 5 mM KPi (pH 7.4) for 1 h in advance of the assay. The authors concluded that the reason for this apparent loss of cytochrome *c* reductase activity was that the dimeric form of flavocytochrome P450 BM3 was required not only for fatty acid hydroxylation (through the heme cofactor), but also for cytochrome *c* reduction (via the FMN cofactor in the CPR domain) [15]. While we were able to replicate the cytochrome *c* activity loss results of Kitazume et al. using their assay conditions (and also in 50 mM KPi, pH 7.4), there is a notable difference in the outcome of this experiment by comparison to similar studies done previously [12]. In our earlier work, Neeli et al. also investigated the influence of dilution of P450 BM3 on the cytochrome *c* reductase specific activity, and found that there was only a small decrease in the specific activity at the lowest enzyme concentrations tested. In contrast, there were substantial decreases in P450 BM3's specific activity for lauric acid-dependent NADPH oxidation as the enzyme concentration was decreased below 20 nM in the assay. Neeli et al. concluded that the most logical explanation for P450 BM3 activity loss was the dissociation of its dimer into monomers inactive in fatty acid hydroxylation in the concentration range below 20 nM [12]. However, in this earlier paper, we also

highlighted that the FMN cofactor is relatively weakly bound to P450 BM3, and performed supplementation of the assay mixtures with FMN (250 nM) in attempts to ensure that enzyme remained replete with FMN, finding that this treatment did not result in recovery of BM3 fatty acid hydroxylase activity. The experimental approach of Kitazume et al. also varied from the one reported in Neeli et al. in terms of the extensive incubation period for the diluted (10 nM to 3 μ M) P450 BM3 of 1 h prior to assay, and the use of a weak buffer system for the incubation step and enzyme assay (5 mM KPi, pH 7.4) [12,15]. In view of these differences in approach, we considered that dissociation of the FMN cofactor from P450 BM3 could occur during the prolonged incubations of highly dilute enzyme samples performed prior to the cytochrome *c* reduction experiments by Kitazume et al., and that this could lead to loss of the activity as a consequence of the bound FMN being an obligate requirement for efficient electron transfer to cytochrome *c* [15]. Thus, we replicated the conditions of Kitazume et al. and examined the flavin fluorescence in samples of P450 BM3 and its CPR domain incubated for 1 h at concentrations between 25 nM to 3 μ M, with all samples then diluted to 25 nM and fluorescence spectra read immediately.

The results in Fig. 6 (main panel) show the increase in flavin-specific fluorescence for these 25 nM samples of WT P450 BM3 and its CPR domain, with data collected following the 1 h incubations at the indicated protein concentration. The data are corrected to show the maximal percentage change in fluorescence (recorded in the samples pre-incubated at 25 nM for both P450 BM3 and CPR) as 100%, and relative to that for the lowest fluorescence signal in each data set as 0%. In this way, the data for the P450 BM3 and CPR domains can be directly overlaid, revealing the same pattern of progressively increasing flavin fluorescence in those 25 nM enzyme samples derived from stock solutions of WT P450 BM3/CPR domain incubated for 1 hour at 750 nM or less. The inset in Fig. 6 shows an example of the difference in flavin fluorescence between samples of P450 BM3 pre-incubated at 2 μ M (lower spectrum) and 25 nM (upper spectrum) for 1 h, prior to dilution and immediately reading fluorescence emission at a protein concentration of 25 nM. The increased fluorescence originates from free FMN that dissociates from the enzyme incubated at 25 nM, and as a consequence of the K_d for FMN binding being in the same range as that in which the enzymes are pre-incubated. In related work, we have established (from fluorescence quenching studies) that the FMN K_d for its domain in P450 BM3 is \sim 90 nM (Waltham, T.N., Ph.D. thesis, University of Manchester, UK). The fluorescence data sets for both the intact WT P450 BM3 and its CPR domain are highly similar, and show a midpoint for fluorescence change of \sim 100 nM, consistent

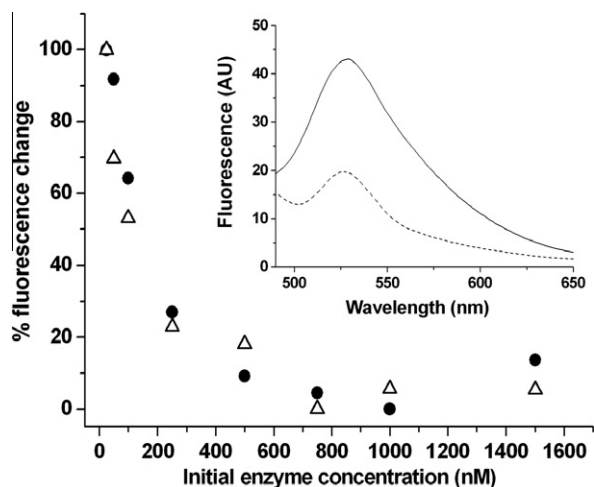


Fig. 6. FMN dissociation from WT flavocytochrome P450 BM3 and its CPR domain on extended incubation at low protein concentration. The main panel shows the proportional increase in flavin fluorescence from samples of WT flavocytochrome P450 BM3 (filled circles) and WT BM3 reductase (CPR) domain (open triangles) in samples pre-incubated at the indicated protein concentration for 1 h in 5 mM KPi buffer (pH 7.4), and prior to dilution to 25 nM in the same buffer for fluorescence measurements. The sample with lowest flavin fluorescence in each group was set to 0% and the sample with highest fluorescence (the samples pre-incubated at 25 nM in both cases) was set to 100%. This allowed the direct overlay of the data sets for P450 BM3 and CPR domain samples. The specific flavin fluorescence was relatively constant in the BM3 and CPR domain samples pre-incubated in the range from ~750 nM to 3 μ M, but increased progressively in samples pre-incubated at lower concentrations, due to dissociation of FMN from the proteins. The midpoint (50% value) occurs at ~100 nM in both cases, consistent with the FMN K_d for the BM3 enzyme. The inset shows flavin fluorescence spectra for samples of WT P450 BM3 pre-incubated at protein concentrations of 2 μ M (dashed line) and 25 nM (solid line), with fluorescence measurements made at an enzyme concentration of 25 nM in both cases.

with the predicted FMN K_d . Subsequent to taking fluorescence readings of the P450 BM3 and CPR domain samples, all were transferred to sealed Eppendorf tubes and boiled for 10 min, prior to centrifugation to pellet debris and cooling to 25 $^{\circ}$ C prior to re-determining flavin fluorescence as before. In all cases, flavin fluorescence increased to approximately the same level (no more than 10% greater) than that for the relevant intact protein samples whose fluorescence was measured after 1 h incubation at 25 nM. This is consistent with both the complete removal of FMN by heat denaturation of the protein samples, and with the much lower fluorescence of FAD (~9-fold) due to quenching from its adenine ring [34]. Thus, we conclude that loss of specific activity of P450 BM3 and its CPR domain in cytochrome *c* reduction likely arises predominantly from dissociation of the crucial FMN cofactor on extended enzyme incubation at concentrations less than ~1 μ M, rather than from dissociation of a P450 BM3 (or CPR domain) dimer into monomers [15]. These data are discussed further in the Discussion section below.

Discussion

The flavocytochrome P450 BM3 system has been studied for more than 30 years following the recognition of a ω -2 palmitic acid hydroxylase activity in cell extracts of *B. megaterium* [27]. The activity was subsequently shown to reside on a 119 kDa enzyme formed from the fusion of a soluble P450 hemoprotein to the first recognized example of a soluble, bacterial CPR enzyme [8,35]. Like eukaryotic CPR enzymes, BM3 shows a strong preference for NADPH over NADH as its reducing coenzyme, although there has been interest in engineering the BM3 CPR domain to facilitate tighter binding of NADH and to switch selectivity towards this cheaper

coenzyme [18]. Point mutations at residue Trp1046 (whose side chain covers the *re*-face of the BM3 FAD isoalloxazine ring) had spectacular effects on coenzyme selectivity in BM3, improving the NADH K_m >250-fold in cytochrome *c* reductase reactions by the W1046A BM3 CPR domain (from 12.8 mM to ~50 μ M) and improving its catalytic efficiency (k_{cat}/K_m) with NADH by ~2200-fold [18]. This paper provides a detailed characterization of the catalytic capacity of the W1046A mutant of the intact flavocytochrome P450 BM3, and demonstrates that the enzyme is a competent fatty acid hydroxylase using both NADPH and NADH as reducing coenzymes, but with rather greater efficiency in lauric acid hydroxylation using NADH. We also demonstrate here that the WT P450 BM3 enzyme is active in lauric acid hydroxylation using NADH, although the activity is weaker than that of the W1046A mutant with NAD(P)H (Fig. 5). Nonetheless, this demonstrates clearly that consecutive NADH-dependent electron transfers occur between the CPR domain FMN cofactor and the BM3 heme iron (in both WT and the W1046A mutant) in order to generate a reactive ferryl-oxo species (compound 1) that catalyzes the hydroxylation reaction. In addition, the regioselectivity of lauric acid hydroxylation (ω -1, ω -2, and ω -3 hydroxylauric acid products formed) is retained with both NADH and NADPH as reductants and in both WT/W1046A BM3 enzymes, confirming that this is a feature controlled by the heme domain of BM3 itself.

While the proof of NADH-driven fatty acid hydroxylation and enhancement of efficiency of this reaction in the W1046A BM3 enzyme are of interest in their own right and have possible biotechnological ramifications, these data also impact on our models of the electron transfer mechanism in P450 BM3. It is now widely accepted that the dimeric state of the enzyme is the form active in fatty acid hydroxylation [11,12,15]. In 2005, Neeli et al. [12] published evidence for the functional BM3 dimer, concluding that a NOS-like electron transfer pathway from FMN₁-to-heme₂ (and vice versa) was likely, based on the restoration of lauric acid hydroxylase activity in the heterodimer formed between inactive G570D and A264H mutants (Fig. 1). Kitazume et al. then proposed a different model in which electron transfer occurs from FAD₁-to-FMN₂ (and vice versa) with the possibility of electron transfer from FMN to either heme in the dimer, with an assumption made that the W1046A BM3 mutant is inactive in fatty acid hydroxylation [15]. However, their own data set did reveal substantial oxygen consumption by W1046A BM3 in presence of NPG and NADPH (specific rate of ~75 min⁻¹), whereas the W1046A/G570D mutant is essentially devoid of such activity [15]. Our studies reported herein (under similar conditions, but using a substrate-dependent NADPH oxidation assay) indicate quite similar k_{cat} values of 83.5 min⁻¹ (lauric acid) and 172 min⁻¹ (NPG) to the rate reported by Kitazume et al. (Table 1). Klein and Fulco demonstrated previously that the G570D BM3 mutant was completely depleted of FMN and had no myristic acid hydroxylase activity [16], a result confirmed by Neeli et al. in studies of lauric acid oxidation [12]. In combination with the results presented in this paper (demonstrating catalytic properties of the W1046A BM3 mutant), it appears clear that the W1046A/G570D mutant is inactive purely as a consequence of the G570D mutation and its effect of preventing FMN binding. Thus, the conclusion that the FAD/NADPH binding domain of P450 BM3 is inactivated in the W1046A mutant is invalid, as shown both by (i) our earlier studies on the catalytic competence of the W1046A FAD/NADPH domain in ferricyanide reduction and of the W1046A CPR domain in cytochrome *c* reduction (also demonstrating efficient FAD-to-FMN electron transfer reactivity in the latter case) [18]; and (ii) by the results presented in this paper which prove that a functional pathway of electron transfer from NAD(P)H through FAD, FMN and onto heme iron occurs in the W1046A BM3 enzyme to support lauric acid (and NPG) hydroxylation. In view of our previous studies of the restoration of

fatty acid hydroxylase activity in the A264H/G570D BM3 heterodimer, this leads to a conclusion (see Fig. 1) that a likely electron transfer pathway in P450 BM3 should be FAD₁-to-FMN₁-to-heme₂, as was postulated for the nitric oxide synthase flavocytochromes [13]. Kitazume et al. suggested that a functional A264H/G570D BM3 heterodimer could be explained by the more complex electron transfer model of FAD₁-to-FMN₂-to-heme₁ [15]. However, inherent in the development of this model was an assumption that the W1046A mutation inactivates P450 BM3. In this paper we show W1046A BM3 to be a functional fatty acid hydroxylase with NAD(P)H coenzymes.

However, Kitazume et al. also considered amino acid sequence alignments of P450 BM3 and related flavocytochromes with those of mammalian CPR enzymes, pointing out that the peptide regions that likely form the “linker” between the FMN and FAD/NADPH domains are shorter in the former group. The question was thus raised as to whether a BM3-type linker was sufficiently long to enable intra-monomer electron transfer (FAD₁-to-FMN₁), whereas inter-monomer electron transfer might be favoured (FAD₁-to-FMN₂) [15]. The crystal structure of rat CPR provided a paradigm for this family of diflavin reductase enzymes [36]. The modular structure of CPR revealed the evolutionary adaptations made in this type of ferredoxin NADP⁺-reductase (FNR)/flavodoxin (FLD) fusion enzyme that enable the close docking of these domains to facilitate the close approach of their FAD and FMN cofactors. In the CPR structure of Wang et al., the FAD and FMN isoalloxazine rings are separated by only ~4 Å, entirely consistent with direct interflavin electron transfer within a CPR monomer [36]. While different conformations of the domains are clearly required in rat CPR (and other diflavin reductases) to enable the reduced FMN-binding domain to move away from its FAD/NADPH domain partner and to communicate with a P450 protein, it is not immediately obvious why the electron transfer system in P450 BM3 should be different from that in rat CPR and instead require cross-interactions of flavin domains across the dimer (FAD₁ with FMN₂ and vice versa). In recent studies, we have determined the crystal structure of the BM3 FAD/NADPH binding domain (Joyce, M.G., Ph.D. thesis, University of Leicester, UK) and we thus examined its interactions with the FMN-binding domain of P450 BM3 [37]. We conclude that, in absence of specific knowledge on the relative docking orientations of these BM3 domains and the precise domain boundaries, no robust conclusion can yet be drawn in favor of either an intra-monomer (FAD₁-to-FMN₁) or inter-monomer (FAD₁-to-FMN₂) electron transfer pathway. However, it is clear that the same type of inter-domain interface as formed in rat CPR is also feasible between BM3 FAD/NADPH and FMN domains, placing the flavin isoalloxazine dimethyl groups in close proximity. In absence of compelling structural evidence to the contrary, we consider the CPR-like intra-monomer electron transfer model most likely for P450 BM3 (FAD₁-to-FMN₁). Thus, a model of P450 BM3 electron transfer consistent with our data sets (and in light of the catalytic competence of W1046A BM3) is FAD₁-to-FMN₁-to-heme₂ (Fig. 1). While we cannot rule out that an electron transfer pathway can occur entirely within one monomer of the BM3 dimer (i.e. FAD₁-to-FMN₁-to-heme₁), we favor the NOS-like FAD₁-to-FMN₁-to-heme₂ scheme based on data presented in this paper and in our previous study [12].

A further consideration with respect to rationalizing the functional properties of P450 BM3 in its dimeric form also emerged from earlier studies of Kitazume et al., where loss of cytochrome *c* reductase activity was observed in P450 BM3 samples incubated for 1 h at low protein concentrations. It was suggested that this phenomenon may reflect the separation of the BM3 dimer. While such changes in dimer–monomer equilibrium are likely to occur at the lower end of the spectrum of protein concentrations used in their study, we were uncertain of the validity of a conclusion

that the BM3 monomer should be inactive in cytochrome *c* reduction, given that the monomeric forms of eukaryotic CPR enzymes are almost certainly proficient catalysts of cytochrome *c* reduction and since our data herein are consistent with interflavin electron transfer within a BM3 monomer (i.e. FAD₁-to-FMN₁). However, formation of monomers inactive in cytochrome *c* reduction would be consistent with a model of obligate FAD₁-to-FMN₂ electron transfer that could be peculiar to the BM3-type system. That said, an alternative explanation for the loss of P450 BM3 cytochrome *c* reductase activity following extended incubations of P450 BM3 enzyme at concentrations of 1 μM and lower would be that the more weakly bound flavin cofactor (the FMN) dissociates from the enzyme, disrupting the obligatory pathway of electron transfer from protein-bound FMN to cytochrome *c*. The data shown in Fig. 6 show this to be the case, with enhanced flavin fluorescence in both WT P450 BM3 (and BM3 CPR) samples incubated at concentrations <750 nM occurring as a consequence of FMN dissociation from its protein binding site and into the surrounding buffer. Thus, data collected in this study suggest that loss of cytochrome *c* reductase activity in highly diluted samples of P450 BM3 and its CPR domain results primarily from loss of the FMN cofactor required as a conduit of electrons to the cytochrome *c* heme, and is probably unrelated to monomerization of the enzymes.

Conclusion

The data presented in this manuscript demonstrate clearly that the W1046A mutant of flavocytochrome P450 BM3 is a catalytically competent fatty acid hydroxylase exhibiting regioselectivity of lauric acid hydroxylation the same as that observed for the WT P450 BM3 enzyme. W1046A P450 BM3 is shown to be active with both NADH and NADPH coenzymes, and to favor slightly NADH in terms of quantities of hydroxylauric acid products formed in unit time (Figs. 4 and 5). These data are consistent with our previous studies to engineer catalytic efficiency with NADH into the W1046A BM3 reductase and FAD/NADPH domain enzymes [18], and have potential biotechnological applications for the exploitation of the P450 BM3 W1046A mutant in NADH-dependent substrate oxidations. Importantly, the WT P450 BM3 enzyme was also shown to catalyze NADH-dependent lauric acid hydroxylation, albeit with much lower efficiency than WT BM3 with NADPH as reductant, or than W1046A BM3 with NAD(P)H. These findings lead to a re-evaluation of models of electron transport within the P450 BM3 dimer, and are consistent with our previous model of electron transfer from NAD(P)H occurring to FAD then FMN within monomer 1 of the dimer, but then from this FMN to the heme iron in monomer 2 of the dimer, as is also postulated to occur in NOS enzymes.

Acknowledgment

This work was supported by research grant awards from the Biotechnology and Biological Sciences Research Council, UK (grant numbers BB/F00252/1 and BB/F00883X1).

References

- [1] I.G. Denisov, T.M. Makris, S.G. Sligar, I. Schlichting, *Chem. Rev.* 105 (2005) 2253–2277.
- [2] A.W. Munro, H.M. Girvan, K.J. McLean, *Nat. Prod. Rep.* 24 (2007) 585–609.
- [3] K.J. McLean, A.W. Munro, *Drug Metab. Rev.* 40 (2008) 427–446.
- [4] S.M. Paquette, K. Jensen, S. Bak, *Phytochemistry* 70 (2009) 1940–1947.
- [5] E.P. Neve, M. Ingelman-Sundberg, *Curr. Opin. Drug Discov. Devel.* 13 (2010) 78–85.
- [6] T.L. Poulos, *Biochem. Biophys. Res. Commun.* 312 (2003) 35–39.
- [7] A.W. Munro, D.G. Leys, K.J. McLean, K.R. Marshall, T.W. Ost, S. Daff, C.S. Miles, S.K. Chapman, D.A. Lysek, C.C. Moser, C.C. Page, P.L. Dutton, *Trends Biochem. Sci.* 27 (2002) 250–257.

- [8] L.O. Narhi, A.J. Fulco, *J. Biol. Chem.* 261 (1986) 7160–7169.
- [9] M.A. Noble, C.S. Miles, S.K. Chapman, D.A. Lysek, A.C. MacKay, G.A. Reid, R.P. Hanzlik, A.W. Munro, *Biochem. J.* 339 (1999) 371–379.
- [10] Y. Miura, A.J. Fulco, *Biochim. Biophys. Acta* 388 (1975) 305–317.
- [11] S.D. Black, S.T. Martin, *Biochemistry* 33 (1994) 12056–12062.
- [12] R. Neeli, H.M. Girvan, A. Lawrence, M.J. Warren, D. Leys, N.S. Scrutton, A.W. Munro, *FEBS Lett.* 579 (2005) 5582–5588.
- [13] U. Siddhanta, A. Presta, B. Fan, D. Wolan, D.L. Rousseau, D.J. Stuehr, *J. Biol. Chem.* 273 (1998) 18950–18958.
- [14] D.J. Stuehr, J. Santolini, Z.Q. Wang, C.C. Wei, S. Adak, *J. Biol. Chem.* 279 (2004) 36167–36170.
- [15] T. Kitazume, D.C. Haines, R.W. Estabrook, B. Chen, J.A. Peterson, *Biochemistry* 46 (2007) 11892–11901.
- [16] M.L. Klein, A.J. Fulco, *J. Biol. Chem.* 268 (1993) 7553–7561.
- [17] O. Döhr, M.J. Paine, T. Friedberg, G.C. Roberts, C.R. Wolf, *Proc. Natl. Acad. Sci. USA* 98 (2001) 81–86.
- [18] R. Neeli, O. Roitel, N.S. Scrutton, A.W. Munro, *J. Biol. Chem.* 280 (2005) 17634–17644.
- [19] J.S. Miles, A.W. Munro, B.N. Rospendowski, W.E. Smith, J. McKnight, A.J. Thomson, *Biochem. J.* 288 (1992) 503–509.
- [20] H.M. Girvan, K.R. Marshall, R.J. Lawson, D. Leys, M.G. Joyce, J. Clarkson, W.E. Smith, M.R. Cheesman, A.W. Munro, *J. Biol. Chem.* 279 (2004) 23274–23286.
- [21] H.M. Girvan, H.S. Toogood, R.E. Littleford, H.E. Seward, W.E. Smith, I.S. Ekanem, D. Leys, M.R. Cheesman, A.W. Munro, *Biochem. J.* 417 (2009) 65–76.
- [22] O. Roitel, N.S. Scrutton, A.W. Munro, *Biochemistry* 42 (2003) 10809–10821.
- [23] A.W. Munro, S. Daff, J.R. Coggins, J.G. Lindsay, S.K. Chapman, *Eur. J. Biochem.* 239 (1996) 403–409.
- [24] H.M. Girvan, C.W. Levy, P. Williams, K. Fisher, M.R. Cheesman, S.E.J. Rigby, D. Leys, A.W. Munro, *Biochem. J.* 427 (2010) 455–466.
- [25] T.W. Ost, C.S. Miles, J. Murdoch, Y. Cheung, G.A. Reid, S.K. Chapman, A.W. Munro, *FEBS Lett.* 486 (2000) 173–177.
- [26] S.S. Boddupalli, T. Oster, R.W. Estabrook, J.A. Peterson, *J. Biol. Chem.* 267 (1991) 10375–10380.
- [27] Y. Miura, A.J. Fulco, *J. Biol. Chem.* 249 (1974) 1880–1888.
- [28] S.C. Hanley, S. Daff, *Biochem. Biophys. Res. Commun.* 325 (2004) 1418–1423.
- [29] M.B. Murataliev, M. Klein, A.J. Fulco, R. Feyereisen, *Biochemistry* 36 (1997) 8401–8412.
- [30] T. Omura, R. Sato, *J. Biol. Chem.* 239 (1964) 2370–2378.
- [31] H.M. Girvan, D.J. Heyes, N.S. Scrutton, A.W. Munro, *J. Am. Chem. Soc.* 129 (2007) 6647–6653.
- [32] A. Gutierrez, O. Döhr, M. Paine, C.R. Wolf, N.S. Scrutton, G.C. Roberts, *Biochemistry* 39 (2000) 15990–15999.
- [33] S.N. Daff, S.K. Chapman, K.L. Turner, R.A. Holt, S. Govindaraj, T.L. Poulos, A.W. Munro, *Biochemistry* 36 (1997) 13816–13823.
- [34] A.W. Munro, M.A. Noble, *Methods Mol. Biol.* 131 (1999) 25–48.
- [35] L.O. Narhi, A.J. Fulco, *J. Biol. Chem.* 262 (1987) 6683–6690.
- [36] M. Wang, D.L. Roberts, R. Paschke, T.M. Shea, B.S. Masters, J.J. Kim, *Proc. Natl. Acad. Sci. USA* 94 (1997) 8411–8416.
- [37] I.F. Sevrioukova, H. Li, H. Zhang, J.A. Peterson, T.L. Poulos, *Proc. Natl. Acad. Sci. USA* 96 (1999) 1863–1868.
- [38] H.M. Girvan, H.E. Seward, H.S. Toogood, M.R. Cheesman, D. Leys, A.W. Munro, *J. Biol. Chem.* 282 (2007) 564–572.